



## Research paper

## Classification of lyophilised mixtures using multivariate analysis of NIR spectra

Holger Grohgan<sup>a,\*</sup>, Margot Fonteyne<sup>a</sup>, Erik Skibsted<sup>b</sup>, Thomas Falck<sup>c</sup>, Bent Palmqvist<sup>c</sup>, Jukka Rantanen<sup>a</sup><sup>a</sup> Department of Pharmaceutics and Analytical Chemistry, University of Copenhagen, Copenhagen, Denmark<sup>b</sup> Novo Nordisk A/S, CMC Supply, Analytical Support, Måløv, Denmark<sup>c</sup> Novo Nordisk A/S, CMC Supply, Pharmaceutics Biopharm, Gentofte, Denmark

## ARTICLE INFO

## Article history:

Received 26 January 2009

Accepted in revised form 30 June 2009

Available online 3 July 2009

## Keywords:

NIR

Freeze-drying

Multivariate analysis

Excipients

Solid state

## ABSTRACT

Excipient selection is critically affecting the processing and the stability of a lyophilised product. Near infra-red (NIR) spectroscopy was applied to investigate freeze-dried samples containing varying ratios of the commonly used excipients mannitol and sucrose. Further variation in the formulation was achieved by adding NaCl, CaCl<sub>2</sub> and histidine and by exposing the samples to different conditions. Untreated NIR spectra are strongly affected by the physical nature of samples and can thus be useful for detecting production outliers. Applying standard normal variate (SNV) transformation highlights chemical information. The obtained NIR spectra of the freeze-dried samples were clustered by principal component analysis (PCA) after applying SNV correction in the range from 4200 to 7400 cm<sup>-1</sup> (1350–2380 nm). Relative humidity under storage and the mannitol/sucrose ratio were clearly represented in the first two principal components, while influence of other excipients was observed in the 3rd and 4th principal component. It was investigated whether this could be due to an influence of the excipients on the mannitol crystallisation behavior. Performing PCA with two principal components of SNV-corrected spectra in the range 4200–4500 cm<sup>-1</sup> (2220–1380 nm) led to the following observation: while the 1st principal component closely resembled the spectra of β-mannitol, the 2nd principal component contained additional features that were not attributable to β-mannitol but correlated well to the main absorbance band of δ-mannitol and mannitol hemihydrate. Therefore, it seems feasible that NIR can analyse versatile freeze-dried samples and classify these according to composition, water content and solid-state properties.

© 2009 Elsevier B.V. All rights reserved.

## 1. Introduction

There is a greater need for advanced formulation and processing strategies applying the concept of quality by design (QbD) due to an increasing number of biomacromolecules in the pipeline of pharmaceutical companies. As many biomacromolecules are less stable when stored in solution, drying is a necessary step in the processing of a drug formulation. However, it has to be considered that biomacromolecules, besides being prone to stresses caused by chemical substances, are also prone to stresses due to heat. Freeze-drying therefore seems to be the natural choice for the drying of heat-labile substances. Macromolecules also need to be protected from stresses during this unit operation due to (e.g.) cold denaturation, freeze-concentration, pH changes or removal of the bound water layer. Mannitol and sucrose are the two commonly used excipients in the freeze-drying of macromolecules. Besides the

simple ability to act as a bulking agent, mannitol will yield a freeze-dried cake with a high collapse temperature and structural stability; thus, acting as a stabiliser. Sucrose, on the other hand, has been claimed to protect the three dimensional structure and the activity of the protein, e.g., by acting as a substitute after the removal of the water monolayer. Despite their common use and obvious advantages, both mannitol and sucrose do present some challenges in freeze-dried preparations. Firstly, mannitol is known to be able to crystallise in three different polymorphic forms (α, β and δ) as well as mannitol hemihydrate. As crystal bound water might be released under storage from the hemihydrate, it is desirable to avoid the formation of mannitol hemihydrate during freeze-drying. The formation of hemihydrate can be influenced by the freezing as well as the drying conditions and is still influenced by chance due to the stochastic nature of the freezing temperature (super cooling) [1,2]. For instance, it has been reported that annealing can facilitate the formation of δ-mannitol and mannitol hemihydrate [3,4].

Secondly, sucrose, which usually results in an amorphous product upon freeze-drying, will absorb water which leads to deliquescence of the preparation at elevated relative humidities.

\* Corresponding author. Department of Pharmaceutics and Analytical Chemistry, Faculty of Pharmaceutical Sciences, University of Copenhagen, 2100 Copenhagen, Denmark. Tel.: +45 35 33 64 73; fax: +45 35 33 60 30.

E-mail address: [hgr@farma.ku.dk](mailto:hgr@farma.ku.dk) (H. Grohgan).

It can thus be stated that two major issues in the characterisation of freeze-dried samples are the water content and various solid-state properties of the components.

In the recent years, the use of spectroscopic techniques such as near infra-red (NIR) and Raman spectroscopy has increased strongly due to the fast and non-destructive nature of the methods and the possibility to provide real-time information. NIR spectroscopy can provide both chemical and physical information on samples. Physical information will be based on the amount of light scattered and will thus strongly influence the raw spectra. In order to reduce the physical influence on the spectra and to obtain chemical information, mathematical transformation such as derivatives or standard normal variate (SNV) transformation is often performed.

Regarding the determination of water content, NIR has been shown to be a suitable tool due to the strong absorption bands of water (OH stretching and bending combination band at 5100–5300  $\text{cm}^{-1}$ , first overtone of OH stretching at 6800–7100  $\text{cm}^{-1}$ ). In early publications, Derksen [5] and Kamat [6] found a good correlation between the amount of water analysed with NIR and Karl-Fischer titration using large ranges of the NIR spectrum. Recently, narrower ranges of the spectra have been used to describe the state of water. It was shown that NIR can differentiate location and orientation of water in a crystal lattice [7,8]. The potential of NIR to differentiate between surface and bound water due to shifts in the water absorption bands has also been shown [9–11].

Besides the determination of state and amount of water, solid-state properties have been introduced as critical quality parameters. Raman spectroscopy was applied to describe mannitol polymorphic forms for instance [12], and on-line measurements during freeze-drying have been performed [13,14]. NIR has also been applied for on-line freeze-drying measurements [15], and the NIR spectra of  $\alpha$ -,  $\beta$ - and  $\delta$ -mannitol as well as mannitol hemihydrate have been reported [9,13]. The potential of NIR to detect various forms is highly relevant for the quality assurance of lyophilised mannitol products as it has been shown that the freeze-drying conditions can influence the solid-state form in the product [2,16]. Furthermore, several formulation substances have been found to influence the crystallisation behavior of mannitol, e.g. polysorbate 80 [17], glycine and  $\text{Na}_2\text{HPO}_4$  [18], NaCl and alditols [19], or boric acid [20].

The aim of this project was to study whether NIR can be applied for the characterisation of a versatile set of freeze-dried samples. Multivariate analysis of NIR spectra was applied to cluster freeze-dried samples according to critical quality attributes (CQA), i.e. cake collapse, moisture content and variations in the solid-state properties of mannitol.

## 2. Materials and methods

### 2.1. Materials

For this project, mannitol (Unikem, Copenhagen, Denmark), sucrose (Ferro Pfanstiehl, USA), histidine (Alsiano, Kawasaki, Japan), sodium chloride and calcium chloride dihydrate (both: Merck, Darmstadt, Germany) were used.

Samples consisted of 50 mg/ml solutions of various mannitol-sucrose mixtures. The mannitol/sucrose ratio was varied between 0:10, 1:9, 3:7, 5:5, 7:3, 9:1 and 10:0 (w/w). All samples were prepared by pouring 2 ml of the solution into 2 ml borosilicate vials followed by subsequent freeze-drying. In order to achieve samples with a wide span of moisture content, the dried samples were stored at relative humidities (RH) of 0%, 11%, 35% and 75% at room temperature. Besides those binary mixtures, tertiary mixtures were composed containing either 3.2 mg/ml histidine,

2.92 mg/ml NaCl or 1.5 mg/ml  $\text{CaCl}_2$ . A quaternary mixture containing the above-mentioned quantities of both NaCl and histidine was also included. The SNV-corrected spectra of the raw materials are given in Fig. 1.

### 2.2. Methods

#### 2.2.1. Freeze-drying

A pilot-scale Model FCM 10 freeze-dryer (Steris, Cologne, Germany) was used. The freeze-dryer was equipped with a stoppering system and had three shelves and a capacitance as well as a pirani vacuum gauge. The freeze-drying cycle was set up as follows: samples were frozen in the freeze-dryer at  $-45^\circ\text{C}$ . An annealing step of 2 h at a temperature of  $-10^\circ\text{C}$  was included to facilitate the crystallisation of mannitol. Then, the temperature was reduced to  $-45^\circ\text{C}$  again. Primary drying was performed over 60 h at a shelf temperature of  $-28^\circ\text{C}$  and a pressure of 0.05 hPa. Secondary drying was performed at a constant pressure of 0.05 hPa while the temperature was raised linearly to  $+20^\circ\text{C}$  over a period of 8 h and then held constant for another 12 h.

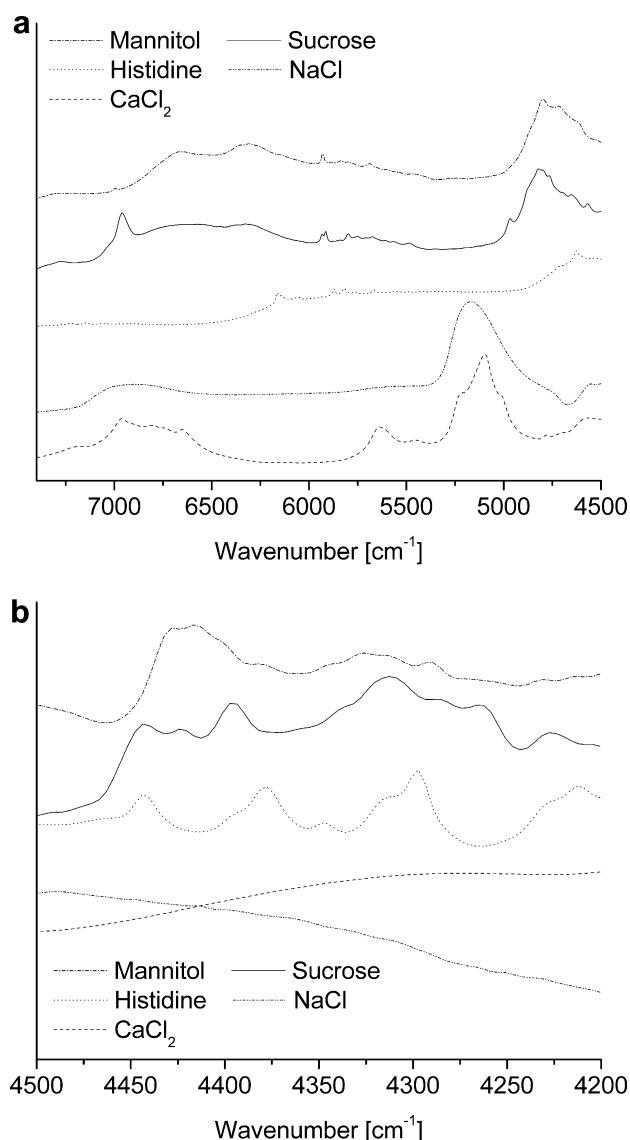


Fig. 1. SNV-corrected NIR spectra of the raw materials: (a) range 7400–4500  $\text{cm}^{-1}$  and (b) range 4500–4200  $\text{cm}^{-1}$ .

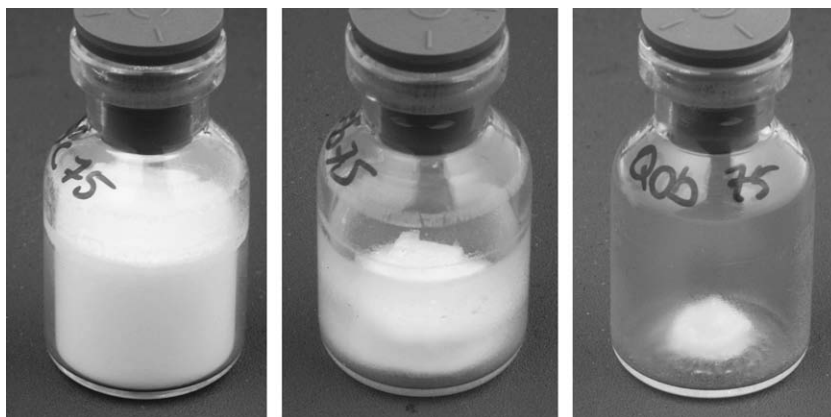


Fig. 2. Examples of freeze-dried samples evaluated as class 1, 3 and 4 (from left to right).

### 2.2.2. NIR analysis

For NIR analysis, a Bomem FTLA 2000 series FT-NIR spectrometer (ABB Bomem, Quebec, Canada) was used. NIR sample measurement was performed through the glass vial. Samples were measured through the side of the vial while placed on a customised spinning device, which rotated the vial perpendicular to the beam of the NIR spectrometer, when the condition of the sample and the remaining filling height allowed this. In cases where measurement through the side was not possible, samples were measured through the bottom of the vial. Due to the large variety in chemical composition and physical appearance of the samples, the slight differences originating from the different measurement set-up can be neglected. Samples were analysed in the range of  $4200\text{--}7400\text{ cm}^{-1}$  with a resolution of  $8\text{ cm}^{-1}$ . A total of 2416 samples were measured.

### 2.2.3. Visual inspection

All freeze-dried samples were assessed visually and categorised into five classes based on their visual appearance, which can be described as follows:

- Class 1: a good cake was obtained. NIR measurement was taken through the side of the vial.
- Class 2: an acceptable cake was obtained. The cake was not always in contact with the wall of the vial. NIR measurement was taken through the side of the vial.
- Class 3: only a shrunken cake remained. The bottom was completely covered with freeze-dried material. NIR measurement was taken through the bottom of the vial.
- Class 4: only a strongly shrunken cake remained. The bottom of the vial was not completely covered with dry material. NIR measurement was taken through the bottom of the vial.
- Class 5: the contents of the vial were deliquescent. NIR measurement was taken through the bottom of the vial.

Exemplary vials of three of those classes are shown in Fig. 2.

### 2.2.4. Data analysis

Obtained NIR spectra were clustered by principal component analysis (PCA) using SIMCA-P 11.5 (Umetrics, Umeå, Sweden). The theoretical background for PCA is widely described in literature and shall therefore not be described in this article. Regarding scaling methods, all NIR spectra were centred. As usual, for spectroscopic data, unit variance scaling was not performed.

## 3. Results and discussion

Both chemical and physical information have to be taken into account and are important for the evaluation of the product when

describing the quality and condition of a system. Preliminary models showed that standard normal variate (SNV) correction is a suitable tool for the interpretation of chemical results. However, before investigating the variation based on chemical changes, the samples were investigated for physical changes. While physical changes can be experienced, for example, in the particle size, the density of the cake or the morphology; in this study, the visual appearance of the cake was investigated as an overall critical quality attribute. For this purpose, the untreated NIR spectra of all samples were analysed by PCA, and the results are given in Fig. 3.

Two trends can be observed in the clustering of the raw data. Firstly, the majority of samples are clustered around the centre of the plot. Secondly, there are several outliers which are widespread over both PC1 and PC2 and lie outside the 95% confidence interval (symbolised by the circle in Fig. 3). Considering the physical heterogeneity of the samples, however, it is obvious that the majority of samples outside correspond to those that have been judged to be of poor quality by visual inspection (classes 4 and 5) and are thus strongly influenced by physical information. It can be seen that samples outside the confidence interval have a high chance of being poor in physical appearance and thus present pharmaceutically unacceptable products. Most of the samples assessed as being in visual class 4 and 5 contained pure sucrose or had a mannitol/sucrose ratio of 1:9. No clustering according to storage time or added excipients was found (data not shown). Fig. 3 shows firstly that measurement through the bottom (e.g. class 3) compared to the side (e.g. class 1 and 2) does not show a clear influence on the spectrum, and secondly that samples with poor visual state can be observed in a PCA plot of the raw data and that they will show a large impact on the model. SNV correction has been shown to remove the interferences from scatter and particle size and thus reduce the influence of the physical information on the spectrum [21]. Therefore, for further interpretation, SNV correction was applied on the range covering the investigated range of the combination bands and first overtones of CH-, NH- and OH-vibrations ( $4200\text{--}7400\text{ cm}^{-1}$ ). The strong influence of physical phenomena for classes 4 and 5 has a high potential for corrupting the model despite SNV correction. For the gathering of chemical information, samples classified to class 4 and 5 by visual inspection have therefore been removed for further processing.

With the physical influence reduced, the clustering based on chemical factors became more visible. Fig. 4a and b shows score plots of PC1 and PC2 for the SNV-corrected data in the range of  $4200\text{--}7400\text{ cm}^{-1}$ , where the colouring<sup>1</sup> was based on relative humidity during storage (Fig. 4a) and mannitol/sucrose ratio

<sup>1</sup> For interpretation of colour in Figs. 1–10, the reader is referred to the web version of this article.

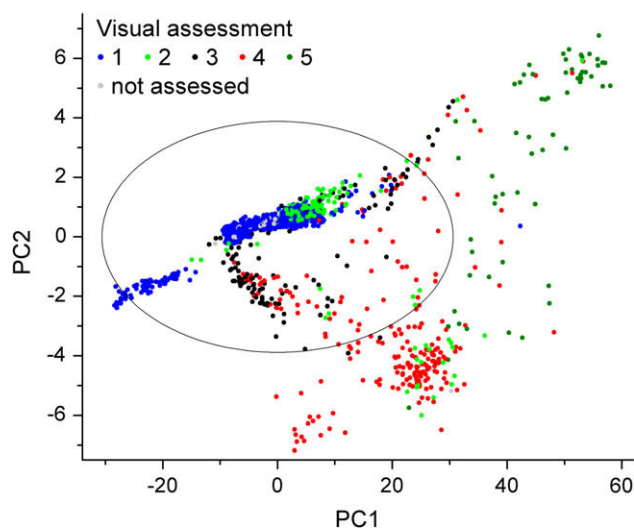


**Fig. 3.** PCA score plot of PC1 against PC2 for untreated data. Spectral range 4200–7400  $\text{cm}^{-1}$  ( $n = 2416$ ). Coloured according to visual inspection.

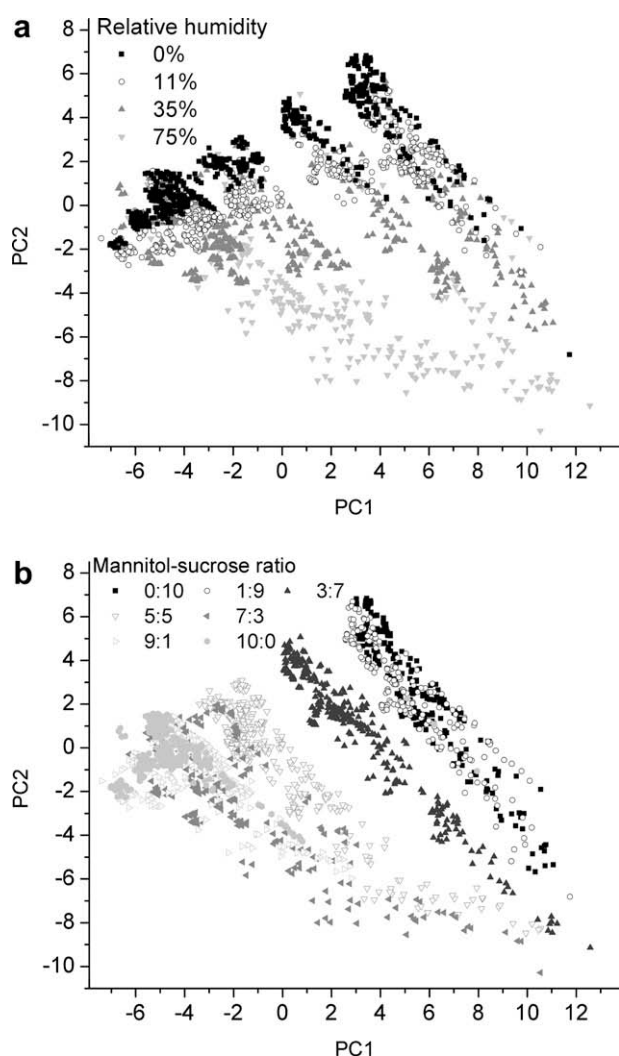


**Fig. 4.** PCA score plot of PC1 against PC2 for SNV-corrected data. Spectral range 4200–7400  $\text{cm}^{-1}$  ( $n = 2088$ ), (a) coloured according to storage humidity and (b) coloured according to mannitol/sucrose ratio.

(Fig. 4b), respectively. Firstly, the influence of storage humidity (Fig. 4a) will be considered, which in turn will influence the water content of the samples. By comparing PC1 and PC2, a clear tendency for samples to move from the 2nd to the 4th quadrant of the Cartesian coordinate system with increasing water content is seen. Furthermore, colouring according to mannitol/sucrose ratio shows that samples move from the 3rd to the 1st quadrant with decreasing mannitol content (Fig. 4b).

It can thus be seen that increasing storage humidity and decreasing mannitol content will result in samples with a more positive PC1 value. Thus, PC1 is based on both the storage humidity and the ratio of the excipients, and the two factors are not independent of each other. This is also apparent in the loadings of PC1 (Fig. 5). The loading plot shows three strong maxima, which can be described as follows:

- (1) maximum at 4900  $\text{cm}^{-1}$  is due to the differences between the R–OH band for mannitol and sucrose,
- (2) maximum at 5165  $\text{cm}^{-1}$  is the combination peak of OH vibrations in water,
- (3) maximum at 6900  $\text{cm}^{-1}$  can represent both the first overtone of the OH band of water and variations in R–OH and CH vibrations between mannitol and sucrose. As these areas commonly overlap a more specific assignment is not possible.

The loadings can be explained from a mechanistic point of view, as mannitol and sucrose will be present in different solids states. Sucrose will have a higher tendency to absorb and retain water, as it is usually in an amorphous state after freeze-drying, while mannitol will crystallise and possibly bind some water as mannitol hemihydrate.

The investigation of the loadings of PC2 shows the same features as for PC1. However, it has to be noted that the water band at 5165  $\text{cm}^{-1}$  shows an even stronger influence in PC2 than in PC1.

Based on the loadings and the clustering in the score plots, it is concluded that the variation in the mannitol/sucrose ratio and the difference in water content are the main factors represented in PC1 and PC2.

It remains to be investigated whether other trends can be seen in the following PCs. As subsequent PCs always show less influence on the model than their preceding PCs, it can be expected that

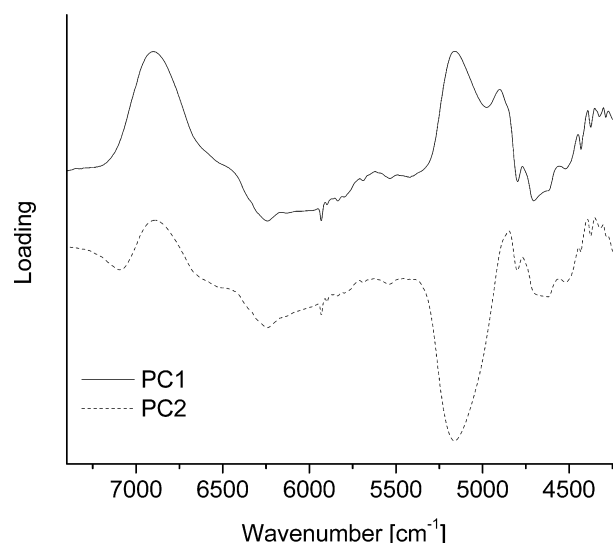


**Fig. 5.** Loading plots of PC1 and PC2 for SNV-corrected data in the spectral range of 4200–7400  $\text{cm}^{-1}$ .



clustering will become less obvious for each new single PC. The score plot of PC3 against PC4 did not show any clustering according to humidity, visual aspects, mannitol/sucrose ratio or storage time. However, with regard to the addition of excipients a certain clustering can be observed (Fig. 6). Although the clustering is less obvious than in Fig. 4a and b, samples containing histidine (coloured green and turquoise) can mainly be found in the upper left segment of the plot. While the binary samples and the samples containing  $\text{CaCl}_2$  (coloured black and red) are spread in the centre of the plot, the samples containing NaCl (coloured blue) can be mainly seen in the lower right segment of the plot.

In order to explain the clustering of PC3 and PC4, the loadings need to be interpreted. In PC3 (Fig. 7), the dominant feature is a peak at  $4800\text{ cm}^{-1}$  which again can be assigned to the R-OH vibration of mannitol and sucrose. The features at  $4713\text{ cm}^{-1}$  as well as  $6680\text{ cm}^{-1}$  cannot be assigned to carbon or oxygen related vibrations, however, they are in the range where combination and first overtone of R-NH<sub>2</sub> vibrations would be expected. The presence of the amino acid histidine in several samples can explain this phenomenon. There are also several bands visible in PC3 and PC4 (Fig. 7) that can be assigned to variations in CH vibrations.

Besides the presence of histidine, there is the question of why NIR-inactive excipients like NaCl and  $\text{CaCl}_2$  should influence the spectrum. The reason may be as follows: it has been reported that both NaCl and the amino acid glycine can influence the crystallisation of mannitol [18,19]. Differences in crystallisation behavior can thus result in the formation of, for instance, mannitol hemihydrate, amorphous mannitol and other polymorphic forms of mannitol, which in turn would show differences in the three dimensional microstructure on molecular level of the formulation and thus influence the strength of the C-H bonds. In other words, this means that the excipient itself is not shown in the spectrum. Rather, the excipient leads to changes in the structure of mannitol which are then visible in the loadings.

To further test this hypothesis, the spectral range from  $4200$  to  $4500\text{ cm}^{-1}$  was investigated. This area was chosen for two reasons: firstly, water will not absorb radiation and therefore will not influence the spectra. Secondly, this area was used for the description of the NIR spectra of the four different solid forms, i.e.  $\alpha$ -,  $\beta$ - and  $\delta$ -mannitol as well as mannitol hemihydrate [13]. The score plots of PC1 and PC2 again show a clear clustering according to the mannitol/sucrose ratio. It can be observed that increasing the mannitol content will lead to more positive values on PC1. Furthermore, it

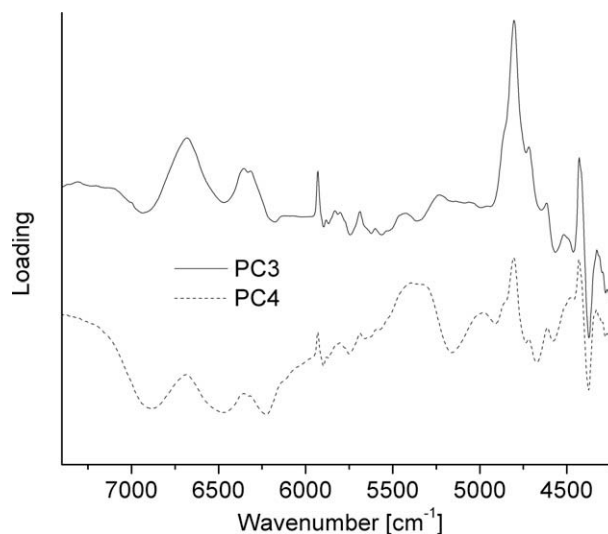


Fig. 7. Loading plots of PC3 and PC4 for SNV-corrected data in the spectral range  $4200\text{--}7400\text{ cm}^{-1}$ .

can be observed that samples are more spread out and drawn from the 4th to the 2nd quadrant with increasing mannitol content. This can be attributed to the variations in PC1 combined with PC2 (Fig. 8).

In order to find an explanation for the scattering, again the loadings will be investigated. A comparison of the loadings of PC1 with the raw spectra of  $\beta$ -mannitol (Fig. 9) reveals a strong correlation between the  $\beta$ -mannitol content and PC1, both showing a strong band at  $4430\text{ cm}^{-1}$  and an elevated area between  $4280$  and  $4360\text{ cm}^{-1}$ . As the starting material was found primarily to be  $\beta$ -mannitol, this resembles the increase of mannitol in the formulation.

So far it remains unclear why the mannitol samples start to spread out as seen in Fig. 8. For a closer investigation of this phenomenon, PC2 will be interpreted. Two of the most prominent features of PC2 are two bands at  $4375\text{ cm}^{-1}$  and  $4430\text{ cm}^{-1}$  (Fig. 10). The band at  $4430\text{ cm}^{-1}$  corresponds well to the maximum absorbance band of  $\beta$ -mannitol shown above. However, the main feature of PC2, the band at  $4375\text{ cm}^{-1}$ , cannot be attributed to  $\beta$ -mannitol. On the other hand, it can be attributed to the main absorbance

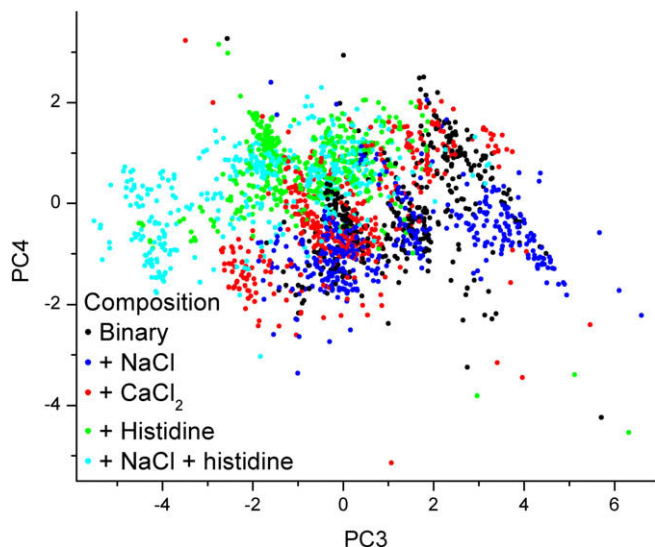


Fig. 6. PCA score plot of PC3 against PC4 for SNV-corrected data. Spectral range  $4200\text{--}7400\text{ cm}^{-1}$  ( $n = 2088$ ). Coloured according to composition.

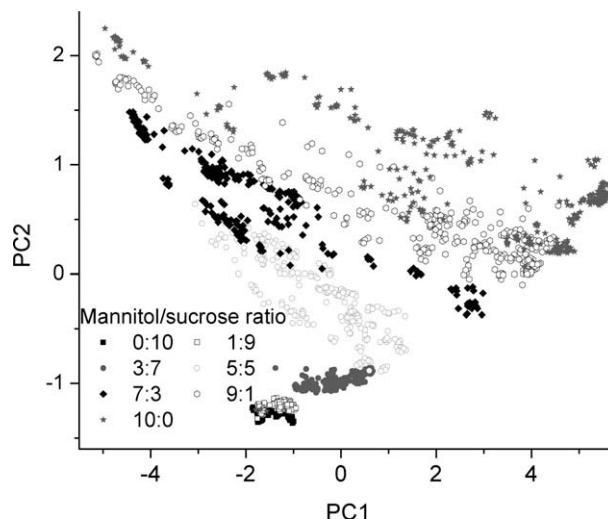


Fig. 8. PCA score plots of PC1 and PC2 of SNV-corrected spectra in the range  $4200\text{--}4500\text{ cm}^{-1}$  ( $n = 2088$ ). Coloured according to mannitol/sucrose ratio.

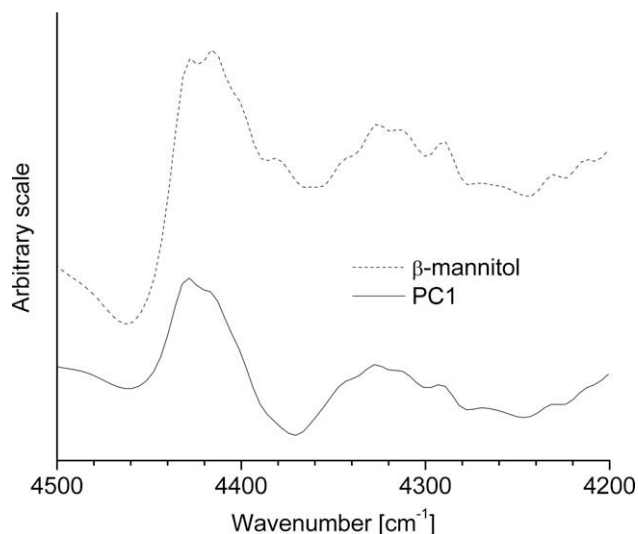


Fig. 9. Comparison between the SNV-corrected spectrum of  $\beta$ -mannitol and the loadings of PC1 (SNV-corrected data in the spectral range of 4200–4500  $\text{cm}^{-1}$ ).

band of mannitol hemihydrate, which can be found at 4375  $\text{cm}^{-1}$ , and thus there is an indication that PC2 is based on variation in both the  $\beta$ -mannitol and the mannitol hemihydrate contents. It has to be mentioned that the NIR spectra of mannitol hemihydrate and  $\delta$ -mannitol are rather similar, so that PC2 might also be attributable to the formation of  $\delta$ -mannitol.

It can be concluded that increasing the mannitol content will lead to a higher score value for PC1 due to the amount of  $\beta$ -mannitol. In addition, increasing the overall content of mannitol in the formulation will increase the risk of the formation of a larger amount of  $\delta$ -mannitol or mannitol hemihydrate. This phenomenon can be the reason for the variation represented in PC2. None of the bands seen in PC1 and PC2 could clearly be attributed to the sucrose.

In order to draw a final conclusion as to whether the formation of mannitol hemihydrate can be observed in such an inhomogeneous sample set, the extensive use of a reference method such as X-ray power diffraction should be applied. In any case, it can be concluded that it is feasible to detect differences in the solid

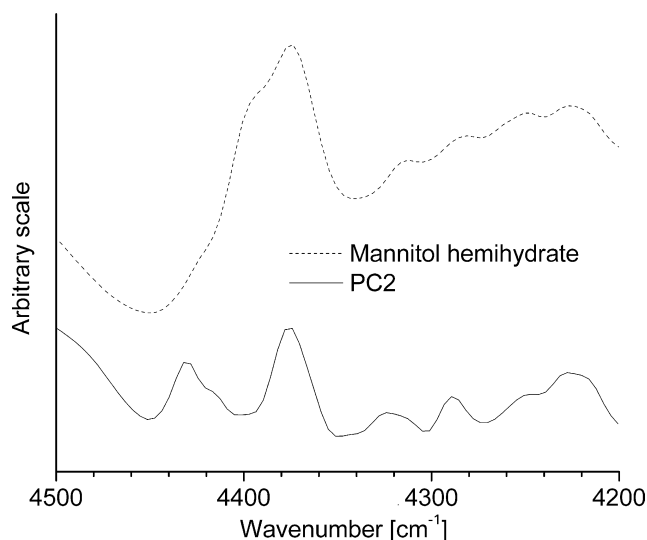


Fig. 10. Comparison between the SNV-corrected spectrum of mannitol hemihydrate (MHH) and the loadings of PC2 (SNV-corrected data in the spectral range 4200–4500  $\text{cm}^{-1}$ ).

state of mannitol in freeze-dried mixtures using SNV-corrected NIR spectra.

#### 4. Conclusions

For fast and reliable quality control of freeze-dried preparations, sensitive analytical techniques with a high capacity and an ability to simultaneously investigate several quality parameters are required. An ideal solution would reduce the time used for end product testing and enable real-time release of a batch. It has been shown that NIR spectroscopy can be used to detect and cluster freeze-dried samples containing mannitol, sucrose and several other excipients according to various factors such as storage humidity (moisture content), mannitol/sucrose ratio, visual appearance and the influence of excipients; thus, providing such an analytical tool. By focussing on the wavenumber range between 4200 and 4500  $\text{cm}^{-1}$ , it seems feasible to cluster highly varying samples based on the presence of different solid-state forms of mannitol.

#### Acknowledgement

The authors would like to thank Thomas de Beer (University of Ghent) for the provision of mannitol NIR reference spectra.

#### References

- [1] C. Nunes, R. Suryanarayanan, C.E. Botez, P.W. Stephens, Characterization and crystal structure of  $\alpha$ -mannitol hemihydrate, *J. Pharm. Sci.* 93 (2004) 2800–2809.
- [2] L. Yu, N. Milton, E.G. Groleau, D.S. Mishra, R.E. Vansickle, Existence of a mannitol hydrate during freeze-drying and practical implications, *J. Pharm. Sci.* 88 (1999) 196–198.
- [3] J.R. Beattie, L.J. Barrett, J.F. Malone, J.J. McGarvey, M. Nieuwenhuyzen, V.L. Kett, Investigation into the subambient behavior of aqueous mannitol solutions using temperature-controlled Raman microscopy, *Eur. J. Pharm. Biopharm.* 67 (2007) 569–578.
- [4] X. Liao, R. Krishnamurthy, R. Suryanarayanan, Influence of processing conditions on the physical state of mannitol-implications in freeze-drying, *Pharm. Res.* 24 (2007) 370–376.
- [5] M.W.J. Derksen, P.J.M. Van De Oetelaar, F.A. Maris, The use of near-infrared spectroscopy in the efficient prediction of a specification for the residual moisture content of a freeze-dried product, *J. Pharm. Biomed. Anal.* 17 (1998) 473–480.
- [6] M.S. Kamat, R.A. Lodder, P.P. DeLuca, Near-infrared spectroscopic determination of residual moisture in lyophilized sucrose through intact glass vials, *Pharm. Res.* 6 (1989) 961–965.
- [7] G. Buckton, E. Yonemochi, J. Hammond, A. Moffat, The use of near infra-red spectroscopy to detect changes in the form of amorphous and crystalline lactose, *Int. J. Pharm.* 168 (1998) 231–241.
- [8] W. Dzik, J.F. Bauer, J.J. Szpylman, J.E. Quick, B.C. Nichols, The use of near-infrared spectroscopy to monitor the mobility of water within the sarafloxacin crystal lattice, *J. Pharm. Biomed. Anal.* 22 (2000) 829–848.
- [9] W. Cao, C. Mao, W. Chen, H. Lin, S. Krishnan, N. Cauchon, Differentiation and quantitative determination of surface and hydrate water in lyophilized mannitol using NIR spectroscopy, *J. Pharm. Sci.* 95 (2006) 2077–2086.
- [10] P. Luukkainen, J. Rantanen, K. Makela, E. Rasanen, J. Tenhunen, J. Yliruusi, Characterization of wet massing behavior of silicified microcrystalline cellulose and alpha-lactose monohydrate using near-infrared spectroscopy, *Pharm. Dev. Technol.* 6 (2001) 1–9.
- [11] G.X. Zhou, Z. Ge, J. Dorwart, B. Izzo, J. Kukura, G. Bicker, J. Wyvrat, Determination and differentiation of surface and bound water in drug substances by near infrared spectroscopy, *J. Pharm. Sci.* 92 (2003) 1058–1065.
- [12] Y. Xie, W. Cao, S. Krishnan, H. Lin, N. Cauchon, Characterization of mannitol polymorphic forms in lyophilized protein formulations using a multivariate curve resolution (MCR)-based Raman spectroscopic method, *Pharm. Res.* 25 (2008) 2292–2301.
- [13] T.R.M. De Beer, M. Alleso, F. Goethals, A. Coppens, Y.V. Heyden, H.L. De Diego, J. Rantanen, F. Verpoort, C. Vervaet, J.P. Remon, W.R.G. Baeyens, Implementation of a process analytical technology system in a freeze-drying process using Raman spectroscopy for in-line process monitoring, *Anal. Chem.* 79 (2007) 7992–8003.
- [14] S. Romero-Torres, H. Wikstrom, E.R. Grant, L.S. Taylor, Monitoring of mannitol phase behavior during freeze-drying using non-invasive Raman spectroscopy, *PDA J. Pharm. Sci. Technol.* 61 (2007) 131–145.
- [15] M. Bruells, S. Folestad, A. Sparen, A. Rasmuson, In-situ near-infrared spectroscopy monitoring of the lyophilization process, *Pharm. Res.* 20 (2003) 494–499.

- [16] A.I. Kim, M.J. Akers, S.L. Nail, The physical state of mannitol after freeze-drying: effects of mannitol concentration, freezing rate, and a noncrystallizing cosolute, *J. Pharm. Sci.* 87 (1998) 931–935.
- [17] R. Haikala, R. Eerola, V.P. Tanninen, J. Yliruusi, Polymorphic changes of mannitol during freeze-drying: effect of surface-active agents, *PDA J. Pharm. Sci. Technol.* 51 (1997) 96–101.
- [18] A. Pyne, K. Chatterjee, R. Suryanarayanan, Solute crystallization in mannitol-glycine systems-implications on protein stabilization in freeze-dried formulations, *J. Pharm. Sci.* 92 (2003) 2272–2283.
- [19] C. Telang, L. Yu, R. Suryanarayanan, Effective inhibition of mannitol crystallization in frozen solutions by sodium chloride, *Pharm. Res.* 20 (2003) 660–667.
- [20] T. Yoshinari, R.T. Forbes, P. York, Y. Kawashima, Crystallization of amorphous mannitol is retarded using boric acid, *Int. J. Pharm.* 258 (2003) 109–120.
- [21] R.J. Barnes, M.S. Dhanoa, S.J. Lister, Standard normal variate transformation and de-trending of near-infrared diffuse reflectance spectra, *Appl. Spectrosc.* 43 (1989) 772–777.